

Mott Quantum Criticality in the Anisotropic 2D Hubbard Model

Benjamin Lenz,^{1,†} Salvatore R. Manmana,¹ Thomas Pruschke,^{1,*} Fakhre F. Assaad,² and Marcin Raczkowski^{2,3,‡}

¹*Institute for Theoretical Physics, University of Göttingen, Friedrich-Hund-Platz 1, D-37077 Göttingen, Germany*

²*Institute for Theoretical Physics and Astrophysics, University of Würzburg, Am Hubland, D-97074 Würzburg, Germany*

³*Department of Physics and Arnold Sommerfeld Center for Theoretical Physics, Ludwig-Maximilians-Universität München, D-80333 München, Germany*

(Received 3 September 2015; published 26 February 2016)

We present evidence for Mott quantum criticality in an anisotropic two-dimensional system of coupled Hubbard chains at half-filling. In this scenario emerging from variational cluster approximation and cluster dynamical mean-field theory, the interchain hopping t_{\perp} acts as a control parameter driving the second-order critical end point T_c of the metal-insulator transition down to zero at $t_{\perp}^c/t \approx 0.2$. Below t_{\perp}^c , the volume of the hole and electron Fermi pockets of a compensated metal vanishes continuously at the Mott transition. Above t_{\perp}^c , the volume reduction of the pockets is cut off by a first-order transition. We discuss the relevance of our findings to a putative quantum critical point in layered organic conductors, whose location remains elusive so far.

DOI: 10.1103/PhysRevLett.116.086403

A subject of strong current interest in condensed matter physics is the metal-insulator transition (MIT) [1] with a low critical end point T_c at which the Mott transition ceases to be first order [2–4]. The nature of this critical end point and its universality class is a long-standing issue. From general considerations, one expects it to belong to the Ising universality class [5,6], similar to the liquid-gas transition, with the double occupancy playing the role of a scalar order parameter of the transition. A canonical example is three-dimensional (3D) Cr-doped V_2O_3 , where critical exponents extracted from electrical conductivity measurements very close to the critical end point $T_c \approx 450$ K are consistent with the universality class of the 3D Ising model [7]. In contrast, similar experiments on layered κ -type charge-transfer salts with significantly lower $T_c \approx 40$ K have indicated unconventional Mott criticality [8]. They stimulated subsequent experimental studies either objecting the existence of unconventional behavior [9] or supporting it [10]. Theoretical scenarios of the two-dimensional (2D) Mott transition are also controversial, ranging from ordinary Ising universality [11–13] to unconventional critical exponents [14].

Recently, the question of the nature of the 2D MIT transition has been raised again as new experiments on κ -type and palladium dithiolene organic conductors support either unconventional criticality [2] or 2D Ising criticality [3], respectively. As the conductors studied in Ref. [2] possess low- T ground states with various broken symmetries, the unconventional Mott criticality seems to be generic and unrelated to the proximity to symmetry broken states. Instead, the fact that the critical end point T_c is relatively low suggests quantum effects to become important and necessitates a physical picture contrasting the one building on classical phase transitions [15–17]. Furthermore, a

possible support for the 2D Mott quantum criticality comes from the dynamical mean-field theory (DMFT) [18,19], which reveals unexpected scaling behavior of the resistivity curves in the high- T crossover region $T \gg T_c$. A stringent test of the link between this scaling behavior and the quantum criticality appears, however, to be impossible since the latter is masked in the half-filled 2D Hubbard model by the low- T coexistence dome [20–23]. Moreover, various numerical studies find that T_c remains finite also in the presence of lattice frustration [24–30]. Finally, while the effective suppression of T_c can be achieved with disorder, it requires the proper treatment of Anderson localization effects [31–33].

In this Letter, we propose a different route to account for a low critical end point T_c of the MIT. Considering the fact that quantum fluctuations are enhanced in low-dimensional systems with spatial anisotropy, we investigate, using two complementary state-of-the-art numerical techniques, the effect of anisotropic hopping amplitudes and try to locate the putative quantum critical point at $T = 0$ in the phase diagram.

Model and methods.—We study the frustrated Hubbard model on a square lattice with an anisotropic hopping at half-filling:

$$\mathcal{H} = -\sum_{ij,\sigma} t_{ij} c_{i\sigma}^{\dagger} c_{j\sigma} + U \sum_i n_{i\uparrow} n_{i\downarrow} - \mu \sum_{i,\sigma} n_{i\sigma}, \quad (1)$$

with chemical potential μ and Coulomb repulsion U . The hopping t_{ij} is t along the chains and t_{\perp} between the chains. By tuning the ratio t_{\perp}/t from 0 to 1, we bridge the limit of uncoupled one-dimensional (1D) Hubbard chains ($t_{\perp} = 0$) and the isotropic 2D lattice ($t_{\perp}/t = 1$). In order to remove the perfect nesting antiferromagnetic (AFM) instability of the Fermi surface (FS) [34] also in the 2D regime, which

would lead to an insulating state at any finite value of U [35,36], we add geometrical frustration via next-nearest-neighbor hopping $t' = -t_{\perp}/4$.

The results are obtained by two complementary quantum cluster techniques [37], which can both be described within the framework of self-energy functional theory [38]. In the cluster extension of DMFT (CDMFT) [39], a cluster of N_c interacting impurities is dynamically coupled to an effective bath. The impurity problem is solved using the quantum Monte Carlo (QMC) Hirsch-Fye solver and coupling to the bath is determined self-consistently. To also make the study computationally manageable down to the lowest temperature $T = t/40$ in the 2D regime, where the sign problem hampers the usage of the QMC solver on larger clusters, we use a 2×2 plaquette cluster. The 2×2 cluster is a minimal unit cell which allows one to capture both the 1D umklapp scattering process opening a gap in the half-filled band [40] and short-range 2D AFM spin fluctuations. To trace the Mott transition at zero temperature, we use the variational cluster approximation (VCA) [41,42] with a 2×2 cluster and one additional bath site per correlated site as a reference system [22], i.e., an effective eight-site cluster. In VCA, the grand potential Ω is approximated by the self-energy functional (SEF) at its saddle point. As variational parameters, we choose the hybridization V between correlated and bath sites and chemical potentials of the reference system μ' and the lattice system μ , respectively [43].

Phase diagram.—Our main results are summarized in the ground-state phase diagram in Fig. 1. It shows our estimate of the critical interaction strength U_c at which the system undergoes a transition between Mott insulating and metallic phases in the full range between the 1D and 2D regimes. In agreement with the exact Bethe ansatz solution [44] and bosonization approach [45], VCA yields the Mott phase for any $U > 0$ in the 1D limit [46]. As shown in Fig. 1, this changes dramatically upon coupling the chains: single-particle hopping t_{\perp} shifts the critical interaction U_c towards a finite value, thus enabling the interaction-driven MIT. Initially, U_c increases steeply with t_{\perp} and then continues to grow nearly linearly, as expected for the MIT controlled by the ratio of Coulomb interaction to kinetic energy gain. For $t_{\perp}/t > 0.2$, the MIT line is found to be first-order consistent with former studies of the frustrated 2D Hubbard model [24–30]. In contrast, in the strongly anisotropic case with $t_{\perp}/t \leq 0.2$, it marks a smooth metal-insulator crossover down to $T = 0$. This is supported by a systematic reduction of the critical end point T_c identified within CDMFT (see the inset of Fig. 1). All of these aspects consistently suggest that t_{\perp} is a control parameter which tunes the nature of the Mott transition from strong first order in the 2D limit to continuous at $t_{\perp}^c/t \approx 0.2$. We complement the phase diagram by showing the change of the FS topology when tuning t_{\perp} for values of the interaction close to U_c . Two main features come into

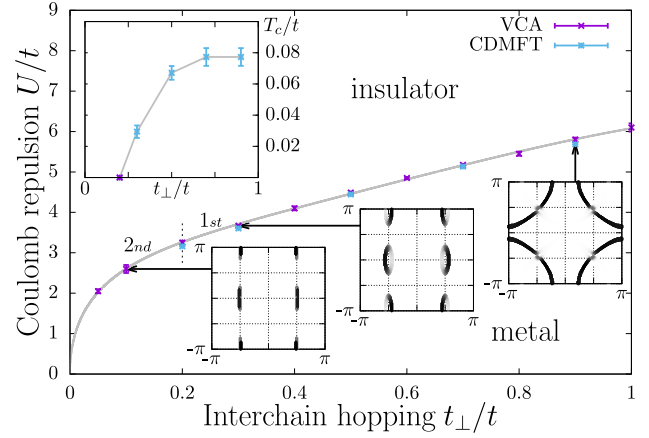


FIG. 1. Metal-insulator phase diagram of the half-filled Hubbard model (1) as obtained by the zero-temperature VCA and CDMFT at $T = t/40$. (Top inset) The combined VCA and CDMFT estimate for the critical temperature T_c terminating the first-order MIT; T_c is driven down to zero at $t_{\perp}^c/t \approx 0.2$, thus providing evidence for the quantum critical nature of the MIT. (Bottom insets) FS topology close to the critical interaction U_c in different regions of the phase diagram indicated by arrows.

play: (i) finite t_{\perp} leads to a warping of the 1D FS and, in the presence of interactions, to the formation of hole and electron Fermi pockets of a higher-dimensional compensated metal [47], and (ii) for values $t_{\perp}/t \gtrsim 0.7$ the compensated metal structure of the FS disappears, going over to a conventional large FS which coincides with the topological Lifshitz transition of the noninteracting FS.

Obtaining the phase diagram.—We now describe the numerical results which lead us to the above phase diagram. VCA provides the possibility of identifying and tracing competing phases by analyzing the self-energy functional $\Omega(\mu, \mu', V)$. For the interchain coupling $t_{\perp}/t = 0.2$, we cannot resolve two disjoint SEF minima and the value of V is thus expected to change continuously across the critical interaction U_c ; see Fig. 2(a). In contrast, for $t_{\perp}/t \gtrsim 0.3$, the SEF has four saddle points, of which two correspond to stable phases close to the phase transition: one corresponding to the metallic, the other to the insulating solution. These stationary points of $\Omega(\mu, \mu', V)$ are maxima with respect to μ and μ' , but minima with respect to hybridization strength V . The existence of two distinct minima in the SEF landscape shown in Fig. 2(b) results in a jump of hybridization V when tuning across U_c , and thus signals the first-order nature of the MIT.

Next, we focus on the ground-state energy E_0 and the double occupancy d . The latter is obtained as the derivative of the grand potential Ω with respect to Coulomb repulsion $d = \partial\Omega/\partial U$. In the quasi-2D region we identify a clear kink in the ground-state energy E_0 ; see Fig. 3(a). It arises from a level crossing of the insulating and metallic solutions and gives rise to a jump in the double occupancy d at U_c , as shown in Fig. 3(b). The latter exhibits hysteresis in the region

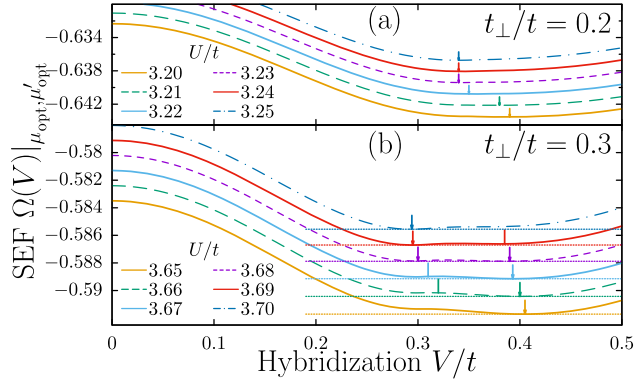


FIG. 2. VCA self-energy functional Ω in the proximity of MIT as a function of hybridization V/t for (a) $t_{\perp}/t = 0.2$ and (b) $t_{\perp}/t = 0.3$. In (b) stable minima are indicated by thick arrows; thinner ones mark unstable solutions.

with two solutions, as expected for the first-order transition. Although a weak kink in E_0 is also resolved for intermediate values of t_{\perp} , both the coexistence region and the jump in the double occupancy shrink and vanish at $t_{\perp}^c/t \approx 0.2$ [48]. The absence of a jump in d and a single minimum in the SEF yield strong evidence for the continuous nature of the MIT. A similar scenario emerges within a finite-temperature CDMFT: while a clear jump in $d = (1/N_c) \sum_i \langle n_{i\uparrow} n_{i\downarrow} \rangle$ is found in the quasi-2D regime, it gradually decreases when reducing t_{\perp} and finally converts into a crossover at $t_{\perp}^c/t = 0.2$. It remains smooth down to our lowest temperature $T = t/40$; see Fig. 3(b). As shown in Fig. 3(c), the level crossing in the ground state is also reflected in the spin sector and produces a jump in the cluster spin susceptibility $\chi_s(\mathbf{q}) = (1/N_c) \int_0^{\beta} d\tau \sum_{ij} e^{i\mathbf{q}\cdot(\mathbf{r}_i - \mathbf{r}_j)} \langle \mathbf{S}_i(\tau) \mathbf{S}_j(0) \rangle$ at the AFM wave vector $\mathbf{q} = (\pi, \pi)$. In contrast, no distinction between the response in $\chi_s(\mathbf{q})$ at $\mathbf{q} = (\pi, 0)$ and $\mathbf{q} = (\pi, \pi)$ wave vectors at $t_{\perp}/t = 0.2$ indicates that remnant 1D effects play an important role in the weakly coupled regime.

We turn now to finite-temperature consequences of the continuous MIT seen at $T = 0$. The estimate of T_c at a given t_{\perp} was obtained by monitoring d as a function of U/t at fixed T ; see Fig. 4. The low- T jump in d signaling the first-order MIT remains up to T_c and turns into a smooth crossover above T_c . As shown in Fig. 4(a), for small $t_{\perp}/t = 0.3$ a smooth behavior in d is already recovered at $T = t/30$. In contrast, for $t_{\perp}/t = 0.9$, the jump converts into a crossover at much higher temperature $T = t/12$. By repeating the above analysis for intermediate values of t_{\perp} , we extracted the t_{\perp} dependence of the critical temperature T_c (see the inset in Fig. 1) consistent with a continuous reduction of the jump in the double occupancy [48].

Spectral function.—To elucidate the microscopic origin of the continuous Mott transition for $t_{\perp}/t \lesssim 0.2$, we calculate the single-particle spectral function $A(\mathbf{k}, \omega) = -(1/\pi) \text{Im}G(\mathbf{k}, \omega)$, where $G(\mathbf{k}, \omega)$ is the lattice Green's function. Figure 5 shows the evolution of $A(\mathbf{k}, \omega)$ upon increasing the interaction U at fixed $t_{\perp}/t = 0.2$.

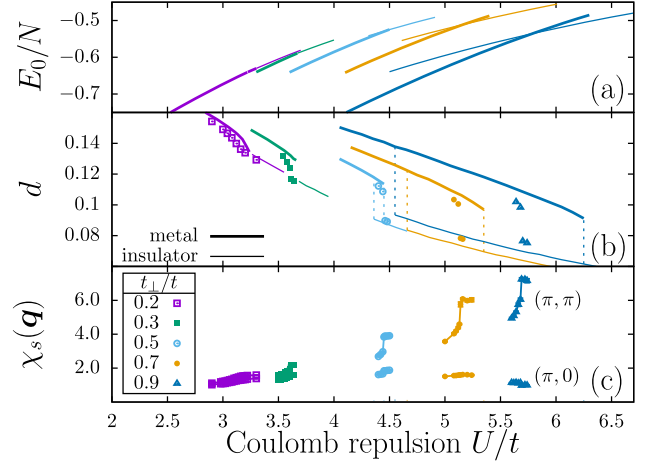


FIG. 3. (a) VCA ground-state energy E_0 as a function of Coulomb repulsion U/t . Filled (dashed) lines indicate metallic (insulating) solutions for $t_{\perp}/t = 0.2, 0.3, 0.5, 0.7$, and 0.9 (from left to right). (b) VCA double occupancy d across the MIT at $T = 0$; symbols stand for CDMFT results at $T = t/40$. (c) Cluster spin susceptibility $\chi_s(\mathbf{q})$ within CDMFT at $T = t/40$; the upper curves correspond to spin fluctuations at the AFM wave vector $\mathbf{q} = (\pi, \pi)$ and the lower ones to remnant 1D fluctuations at $\mathbf{q} = (\pi, 0)$.

In agreement with random-phase approximation studies [50,51], we find that the destruction of the FS starts at momenta $\mathbf{k} = (\pi/2, \pm\pi/2)$, where the interchain hopping matrix elements vanish. As a result, a compensated metal structure of the FS is formed with elliptic electron and hole pockets around the $\mathbf{k} = (\pi/2, 0)$ and $(\pi/2, \pi)$ points. A striking feature of the pockets is their symmetric form contrasted with pockets found in coupled *spinless* fermionic chains [52]. We ascribe this symmetry to quasi-particle scattering off short-range 1D spin fluctuations with $\mathbf{q} = (\pi, 0)$. On one hand, at intermediate interaction strengths, the main part of the FS carrying most of the quasiparticle weight follows closely the noninteracting FS. On the other hand, the pockets shrink in size and become very shallow close to U_c ; see Figs. 6(a)–6(c). The continuous vanishing of the volume of Fermi pockets at U_c implies the second-order nature of the MIT. Since the

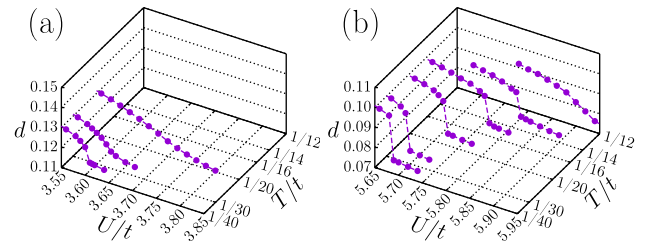


FIG. 4. Double occupancy d as a function of interaction U/t obtained in CDMFT for (a) $t_{\perp}/t = 0.3$ and (b) $t_{\perp}/t = 0.9$. The low- T jump in d signaling the first-order MIT turns into a crossover above the critical end point T_c .

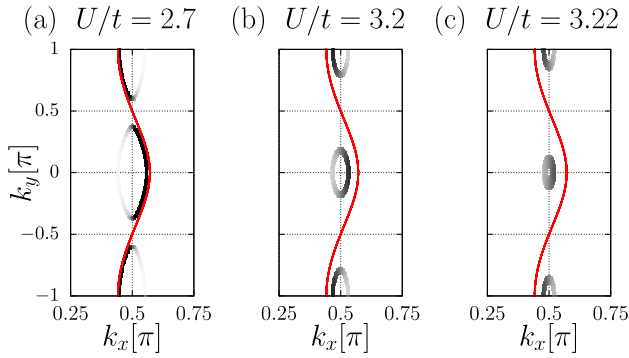


FIG. 5. Evolution of the FS with electron and hole pockets (see the text) for $t_{\perp}/t = 0.2$ when approaching $U_c/t \approx 3.22$ from below: (a) $U/t = 2.7$, (b) $U/t = 3.2$, and (c) $U/t = 3.22$. Red solid lines show the noninteracting dispersion.

inverse width of the hole or electron pockets defines a characteristic length scale, ξ , one should be able to extract the correlation length exponent, ν , from a careful study of the critical behavior of the volume of the pocket as one approaches U_c [1,48]. In contrast, the volume reduction of the pockets is cut off by a first-order transition for larger t_{\perp} ; cf. Figs. 6(d)–6(f) with $t_{\perp}/t = 0.5$.

Discussion and outlook.—Let us relate our findings to recent experiments on the organic conductors with a half-filled band [2]. Both κ -(BEDT-TTF) $_2$ Cu $_2$ (CN) $_3$ and EtMe $_3$ Sb[Pd(dmit) $_2$] $_2$ (BEDT-TTF=bis(ethylenedithio)tetrathiafulvalene, dmit=1,3-dithiole-2-thione-4,5-dithiolate, Me = CH $_3$, Et = C $_2$ H $_5$) are thought to be layered systems with Hückel parameters close to an equilateral triangular lattice [53]. Instead, careful *ab initio* calculations for the latter show an appreciable 1D anisotropy with the ratio of interchain to intrachain transfer around 0.82 [54]

We took this asymmetry into consideration: using VCA at $T = 0$ and CDMFT at finite T , we have found strong evidence for Mott quantum criticality in coupled Hubbard chains at half-filling. In this scenario, the interchain hopping t_{\perp} acts as control parameter driving the second-order critical end point T_c of the interaction-driven MIT down to zero in the presence of strong anisotropy. At a threshold value of $t_{\perp}^c/t \approx 0.2$, the volume of Fermi pockets shrinks to zero. The resulting MIT is without a detectable jump in the double occupancy or a visible coexistence region in the SEF. In contrast, the volume reduction of the pockets is only partial at larger t_{\perp} : the jump in the double occupancy and the existence of two distinct degenerate minima in the SEF are consistent with a first-order transition.

The continuous MIT at $T = 0$ offers a possibility for understanding the scaling behavior of resistivity curves in the high- T crossover region $T \gg T_c$ usually attributed to (hidden) 2D Mott quantum criticality [18,19]. It is an interesting question as to whether the quantum critical behavior emerges also in coupled *spinless* fermionic chains displaying similar FS breakup into Fermi pockets [52].

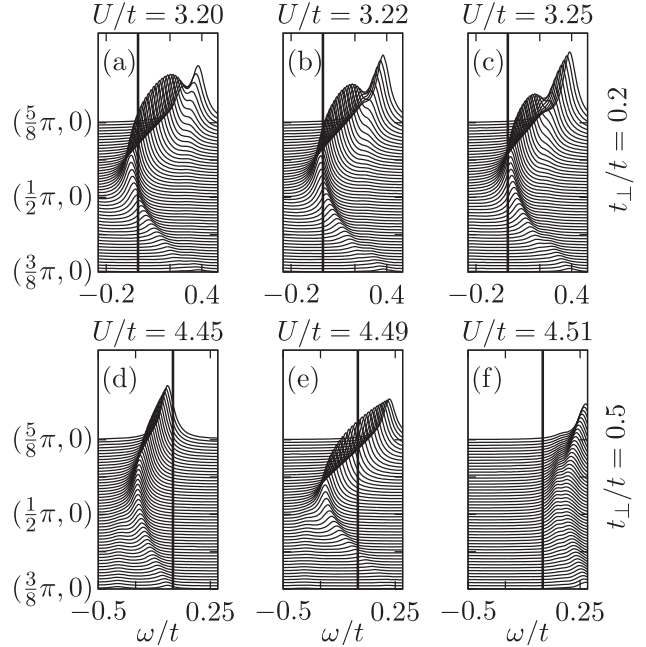


FIG. 6. Low-energy part of the single-particle spectral function $A(\mathbf{k}, \omega + i\eta)$ for $t_{\perp}/t = 0.2$ (top panels) and $t_{\perp}/t = 0.5$ (bottom panels) obtained within VCA at $T = 0$, $\eta = 0.05$. The FS pockets are found (a),(d) for $U < U_c$ and (b),(e) at $U \lesssim U_c$; in the insulator at (c),(f) $U > U_c$, their disappearance signifies the vanishing of the FS, and hence the MIT.

While the 2×2 plaquette cluster used is known to overestimate the singlet formation [37], we expect the unveiled quantum critical behavior to be robust. Indeed, former CDMFT studies on larger clusters of up to 16 sites have provided evidence for a continuous dimensional-crossover-driven MIT down to the lowest accessible temperatures [55]. We believe that this scenario is not restricted to quantum cluster descriptions of the system but should also emerge in lattice simulations, provided that the range of AFM spin fluctuations is reduced, e.g., by geometrical frustration or disorder [56,57]. This leads, however, to a severe sign problem which renders lattice QMC simulations very expensive [58]. In this respect, a promising route avoiding the main shortcomings of QMC is offered by tensor network methods [59] adapted recently to fermionic systems [60,61]. Our results provide a novel axis in the phase diagram along which T_c can be tuned to zero. It remains to be verified if this quantum critical behavior can explain fingerprints of the unconventional Mott criticality observed in layered organic conductors.

We thank M. Imada and A. M. Tsvelik for the insightful discussions. F. F. A. and S. R. M. would like to thank the KITP, where part of this work was carried out, for the hospitality (Grant No. NSF PHY11-25915). We acknowledge the computer support of the GWDG, the GoeGrid project, and the Jülich Supercomputing Centre and financial support from DFG Grants No. PR298/15-1 (FOR

1807) and No. AS120/8-2 (FOR 1346) as well as from FP7/ERC Starting Grant No. 306897.

Note added.—While this manuscript was under review, one of the co-authors, Thomas Pruschke, passed away.

*Deceased.

[†]benjamin.lenz@theorie.physik.uni-goettingen.de

[‡]marcin.raczkowski@physik.uni-wuerzburg.de

- [1] M. Imada, A. Fujimori, and Y. Tokura, *Rev. Mod. Phys.* **70**, 1039 (1998).
- [2] T. Furukawa, K. Miyagawa, H. Taniguchi, R. Kato, and K. Kanoda, *Nat. Phys.* **11**, 221 (2015).
- [3] M. Abdel-Jawad, R. Kato, I. Watanabe, N. Tajima, and Y. Ishii, *Phys. Rev. Lett.* **114**, 106401 (2015).
- [4] B. Hartmann, D. Zielke, J. Polzin, T. Sasaki, and J. Müller, *Phys. Rev. Lett.* **114**, 216403 (2015).
- [5] C. Castellani, C. Di Castro, D. Feinberg, and J. Ranninger, *Phys. Rev. Lett.* **43**, 1957 (1979).
- [6] G. Kotliar, E. Lange, and M. J. Rozenberg, *Phys. Rev. Lett.* **84**, 5180 (2000).
- [7] P. Limelette, A. Georges, D. Jérôme, P. Wzietek, P. Metcalf, and J. M. Honig, *Science* **302**, 89 (2003).
- [8] F. Kagawa, K. Miyagawa, and K. Kanoda, *Nature (London)* **436**, 534 (2005).
- [9] M. de Souza, A. Brühl, C. Strack, B. Wolf, D. Schweitzer, and M. Lang, *Phys. Rev. Lett.* **99**, 037003 (2007).
- [10] F. Kagawa, K. Miyagawa, and K. Kanoda, *Nat. Phys.* **5**, 880 (2009).
- [11] S. Papanikolaou, R. M. Fernandes, E. Fradkin, P. W. Phillips, J. Schmalian, and R. Sknepnek, *Phys. Rev. Lett.* **100**, 026408 (2008).
- [12] L. Bartosch, M. de Souza, and M. Lang, *Phys. Rev. Lett.* **104**, 245701 (2010).
- [13] P. Sémon and A.-M. S. Tremblay, *Phys. Rev. B* **85**, 201101 (2012).
- [14] M. Sentef, P. Werner, E. Gull, and A. P. Kampf, *Phys. Rev. B* **84**, 165133 (2011).
- [15] M. Imada, *Phys. Rev. B* **72**, 075113 (2005).
- [16] T. Misawa and M. Imada, *Phys. Rev. B* **75**, 115121 (2007).
- [17] M. Imada, T. Misawa, and Y. Yamaji, *J. Phys. Condens. Matter* **22**, 164206 (2010).
- [18] H. Terletska, J. Vučičević, D. Tanasković, and V. Dobrosavljević, *Phys. Rev. Lett.* **107**, 026401 (2011).
- [19] J. Vučičević, D. Tanasković, M. J. Rozenberg, and V. Dobrosavljević, *Phys. Rev. Lett.* **114**, 246402 (2015).
- [20] S. Onoda and M. Imada, *Phys. Rev. B* **67**, 161102 (2003).
- [21] H. Park, K. Haule, and G. Kotliar, *Phys. Rev. Lett.* **101**, 186403 (2008).
- [22] M. Balzer, B. Kyung, D. Sénéchal, A.-M. S. Tremblay, and M. Potthoff, *Europhys. Lett.* **85**, 17002 (2009).
- [23] E. Gull, O. Parcollet, P. Werner, and A. J. Millis, *Phys. Rev. B* **80**, 245102 (2009).
- [24] O. Parcollet, G. Biroli, and G. Kotliar, *Phys. Rev. Lett.* **92**, 226402 (2004).
- [25] B. Kyung and A.-M. S. Tremblay, *Phys. Rev. Lett.* **97**, 046402 (2006).
- [26] T. Watanabe, H. Yokoyama, Y. Tanaka, and J.-i. Inoue, *J. Phys. Soc. Jpn.* **75**, 074707 (2006).
- [27] T. Ohashi, T. Momoi, H. Tsunetsugu, and N. Kawakami, *Phys. Rev. Lett.* **100**, 076402 (2008).
- [28] T. Yoshioka, A. Koga, and N. Kawakami, *Phys. Rev. Lett.* **103**, 036401 (2009).
- [29] A. Liebsch, H. Ishida, and J. Merino, *Phys. Rev. B* **79**, 195108 (2009).
- [30] H. T. Dang, X. Y. Xu, K.-S. Chen, Z. Y. Meng, and S. Wessel, *Phys. Rev. B* **91**, 155101 (2015).
- [31] K. Byczuk, W. Hofstetter, and D. Vollhardt, *Phys. Rev. Lett.* **94**, 056404 (2005).
- [32] M. C. O. Aguiar, V. Dobrosavljević, E. Abrahams, and G. Kotliar, *Phys. Rev. B* **71**, 205115 (2005).
- [33] H. Bragança, M. C. O. Aguiar, J. Vučičević, D. Tanasković, and V. Dobrosavljević, *Phys. Rev. B* **92**, 125143 (2015).
- [34] W. Hofstetter and D. Vollhardt, *Ann. Phys. (N.Y.)* **7**, 48 (1998).
- [35] A. H. Nevidomskyy, C. Scheiber, D. Sénéchal, and A.-M. S. Tremblay, *Phys. Rev. B* **77**, 064427 (2008).
- [36] T. Schäfer, F. Geles, D. Rost, G. Rohringer, E. Arrigoni, K. Held, N. Blümer, M. Aichhorn, and A. Toschi, *Phys. Rev. B* **91**, 125109 (2015).
- [37] T. Maier, M. Jarrell, T. Pruschke, and M. H. Hettler, *Rev. Mod. Phys.* **77**, 1027 (2005).
- [38] M. Potthoff, *Eur. Phys. J. B* **32**, 429 (2003).
- [39] G. Kotliar, S. Y. Savrasov, G. Pálsson, and G. Biroli, *Phys. Rev. Lett.* **87**, 186401 (2001).
- [40] M. Capone, M. Civelli, S. S. Kancharla, C. Castellani, and G. Kotliar, *Phys. Rev. B* **69**, 195105 (2004).
- [41] M. Potthoff, M. Aichhorn, and C. Dahnken, *Phys. Rev. Lett.* **91**, 206402 (2003).
- [42] M. Potthoff, *Eur. Phys. J. B* **36**, 335 (2003).
- [43] Note that variation of the hopping terms on the cluster t' and t'_{\perp} did not lead to qualitative differences compared to a variation of μ , μ' and V only. They were therefore chosen to be equal to their lattice analogues and not treated as additional variational parameters.
- [44] E. H. Lieb and F. Y. Wu, *Phys. Rev. Lett.* **20**, 1445 (1968).
- [45] T. Giamarchi, *Quantum Physics in One Dimension* (Oxford University, Oxford, 2004).
- [46] M. Balzer, W. Hanke, and M. Potthoff, *Phys. Rev. B* **77**, 045133 (2008).
- [47] F. H. L. Essler and A. M. Tsvelik, *Phys. Rev. B* **71**, 195116 (2005).
- [48] See Supplemental Material at <http://link.aps.org/supplemental/10.1103/PhysRevLett.116.086403>, which includes Refs. [1,49], for additional numerical evidence of Mott quantum criticality.
- [49] K. S. D. Beach, [arXiv:cond-mat/0403055](https://arxiv.org/abs/cond-mat/0403055).
- [50] F. H. L. Essler and A. M. Tsvelik, *Phys. Rev. B* **65**, 115117 (2002).
- [51] P. Ribeiro, P. D. Sacramento, and K. Penc, *Phys. Rev. B* **84**, 045112 (2011).
- [52] C. Berthod, T. Giamarchi, S. Biermann, and A. Georges, *Phys. Rev. Lett.* **97**, 136401 (2006).
- [53] K. Kanoda and R. Kato, *Annu. Rev. Condens. Matter Phys.* **2**, 167 (2011).
- [54] K. Nakamura, Y. Yoshimoto, and M. Imada, *Phys. Rev. B* **86**, 205117 (2012).

- [55] M. Raczkowski and F.F. Assaad, *Phys. Rev. Lett.* **109**, 126404 (2012).
- [56] K. Byczuk, W. Hofstetter, and D. Vollhardt, *Phys. Rev. Lett.* **102**, 146403 (2009).
- [57] T. Furukawa, K. Miyagawa, T. Ito, M. Ito, H. Taniguchi, M. Saito, S. Iguchi, T. Sasaki, and K. Kanoda, *Phys. Rev. Lett.* **115**, 077001 (2015).
- [58] M. Raczkowski, F.F. Assaad, and L. Pollet, *Phys. Rev. B* **91**, 045137 (2015).
- [59] R. Orús, *Ann. Phys. (Amsterdam)* **349**, 117 (2014).
- [60] P. Corboz and G. Vidal, *Phys. Rev. B* **80**, 165129 (2009).
- [61] P. Corboz, G. Evenbly, F. Verstraete, and G. Vidal, *Phys. Rev. A* **81**, 010303 (2010).